Time-resolved photoluminescence studies of cross-well transport in a biased GaAs/AlGaAs multiple quantum well *p-i-n* structure

J. S. Massa, G. S. Buller, and A. C. Walker
Department of Physics, Heriot-Watt University, Riccarton, Edinburgh EH14 4AS, United Kingdom

(Received 5 February 1997; accepted for publication 7 April 1997)

Time-resolved photoluminescence has been used to study the cross-well carrier dynamics in a biased multiple quantum well *p-i-n* structure at temperatures in the range 5–350 K and for electric fields <200 kV cm^{-1}. The photoluminescence decays have been parameterized using reconvolution analysis with a coupled rate equation model and this has provided strong evidence for the successive recapturing of carriers in adjacent wells. For temperatures <100 K, and for electric fields <60 kV cm^{-1}, the carrier escape appears to be strongly affected by resonant tunneling between hole subbands in adjacent wells. At higher temperatures an increase in the carrier escape rate is observed which corresponds to a field dependent thermal activation energy. © *1997 American Institute of Physics.* [S0021-8979(97)00214-4]

I. INTRODUCTION

The reverse biased multiple quantum well (MQW) *p-i-n* structure is of considerable importance in the design of optoelectronic devices such as detectors, modulators, and self electro-optic effect devices (SEEDs).[1–3] Optimization of such devices for high speed operation, high absorption saturation-irradiance, or low optical switching energy requires a knowledge of the mechanisms responsible for transferring optically injected carriers away from the absorption region and onto the contacts. The use of a MQW structure places a fundamental limitation on the response time of the device, since carriers must first escape from the wells and possibly suffer recapture many times before they finally contribute to the photocurrent. In the past, there have been numerous studies of cross-well transport in GaAs/AlGaAs based low-dimensional structures using both electrical and optical measurement techniques. These have included double barrier[4–7] and double quantum well structures,[8–12] single quantum wells (SQWs),[13] and MQWs' superlattices.[14–19] Despite the large volume of information that has accumulated on this subject, there is still considerable uncertainty about the relative importance of the various carrier escape mechanisms occurring in real devices, particularly at room temperature where operation normally takes place. In this article we present time-resolved photoluminescence (TRPL) measurements and analysis from a reverse biased MQW *p-i-n* diode at temperatures in the range 5–350 K. The aim of this work is to provide further information to help elucidate the processes operating in these devices and to demonstrate the potential of the photon counting technique, with its high statistical accuracy, for this type of study.

II. EXPERIMENTAL DESCRIPTION AND SAMPLE

The measurements were performed on a microscope-based instrument (a derivative of an Edinburgh Instruments Lifemap) which has been described in detail elsewhere.[20] In this work, sample excitation was provided at a wavelength of 780 nm by a passively Q-switched picosecond AlGaAs laser diode (pulse duration <20 ps).[21] The actively quenched single photon avalanche diode (SPAD) detector[22] when coupled with the microscope optical system gives a spatial resolution of <5 μm,[23] and allows TRPL measurements in the spectral range 790–1100 nm. The instrument uses the time-correlated single photon counting (TCSPC) technique[24] and has an instrumental full width at half maximum (FWHM) of 50–60 ps. The samples were mounted in a continuous flow helium cryostat (Oxford Instruments model CF1104) which had been modified to allow close optical access to the sample, thus maintaining the high spatial resolution of the microscope system.

The devices used in these experiments were on a commercial SEED array chip supplied by AT&T Microelectronics. The MQW structure consisted of 71.5 periods of 100 Å GaAs wells with 35 Å $Al_{0.3}Ga_{0.7}As$ barriers. Photoluminescence (PL) decay measurements were performed on 40 μm$\times$40 μm mesa devices, using values of applied bias corresponding to estimated internal fields of up to $\sim$200 kV cm^{-1}, and at temperatures in the range 5–350 K.

III. RESULTS AND RATE EQUATION MODEL

Figure 1 shows a three-axis plot of the PL decay spectrally integrated over the range 845–865 nm, for applied fields between $+10$ and -208 kV cm^{-1}, at room temperature. The peak photogenerated carrier density was $<10^{16}$ cm^{-3} and the excitation spot was sufficiently large, $\sim$15 μm diameter (in the mesa center), to eliminate transverse diffusion effects. The figure shows the expected increase in PL decay rate and decrease in PL intensity as the field across the device is raised—sweeping carriers out of the wells before they can recombine radiatively. Figure 2 shows the PL decay from the structure, spectrally integrated over the peak emission band, at temperatures of 5, 150, and 292 K for a calculated internal field (ignoring local variations due to space charge effects) of 26 kV cm^{-1}. Figure 3 plots the mean PL decay time versus internal field, for temperatures of 5, 100, 200, 292, and 350 K. For both these sets of measurements, wavelength discrimination was provided by interchangeable multiple-cavity bandpass filters centered at 10 nm intervals between 800 and 850 nm and with a passband of $\sim$10 nm (FWHM). Throughout these measurements the selected passband covered the peak of the band-edge/exciton

 0021-8979/97/82(2)/712/6/$10.00 © 1997 American Institute of Physics

Downloaded¬04¬Jun¬2002¬to¬137.195.29.233.¬Redistribution¬subject¬to¬AIP¬license¬or¬copyright,¬see¬http://ojps.aip.org/japo/japcr.jsp

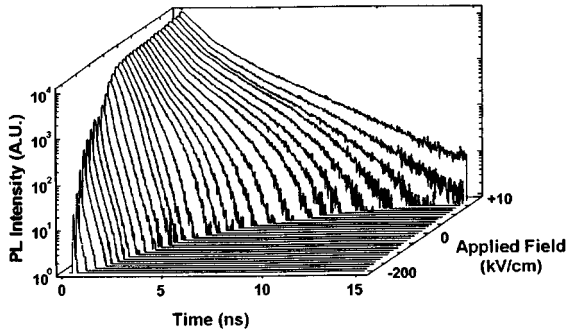

FIG. 1. Room temperature PL decays from a GaAs/AlGaAs MQW *p-i-n* structure as a function of applied field. The decays were taken for the same integration time and thus the peak of each decay represents its peak PL intensity. Note the two separate scales on the applied field axis and that the zero internal field condition is at $\sim +8\ \mathrm{kV\ cm^{-1}}$. Sample excitation was at a wavelength of 780 nm and the PL was collected over the spectral range 845–865 nm. The peak photogenerated carrier density was $<10^{16}\ \mathrm{cm^{-3}}$.

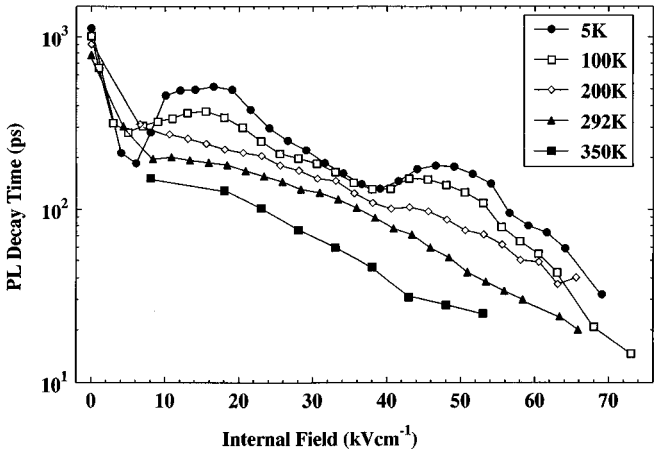

FIG. 3. Mean PL decay time vs internal field at temperatures of 5, 100, 200, 292, and 350 K. The decay times were calculated using an approximate fit to an exponential series. The lines joining the points are as a guide only.

emission. The internal field was calculated by adding the applied field to the in-built field of the *p-i-n* structure. The latter was determined for each temperature by observing the applied field at which the photocurrent changed direction. Figure 4 shows the PL intensity versus electric field for the measurements made at 5 K. It is apparent that both the PL decay time and the PL intensity decrease with increasing internal field and increasing temperature. In addition, the low temperature measurements display minima at particular fields, characteristic of resonant tunneling effects.

The best-fit exponential decay times plotted in Fig. 3, while providing an indication of the consequences of the sweepout process, do not link the PL decay to the underlying dynamical processes occurring in these structures. The PL decay from a device with this structure, when measured over many decades of intensity, cannot be fitted by a single or multiple exponential function but has a decay rate which increases with time after the initial excitation pulse. This nonexponential nature is clearly evident over the first nanosecond of the PL decays shown in Fig. 2, before the decay rate approaches a constant limiting value. The high sensitivity of the TCSPC technique gives a signal dynamic range of typically $>10^4$ and thus, in principle, allows the carrier dynamics to be followed with considerable accuracy over several decades in carrier density. To this end, further analysis was performed by fitting the data to a simple physical model, using reconvolution analysis to eliminate the system response from the rapidly decaying PL signal. The model makes no assumptions about the dominant carrier escape mechanism from the wells but is merely intended to parametrize the full PL decay measured under each set of experimental conditions in terms of the evolving carrier distributions.

As a first approximation, for the low photogenerated carrier densities used in these experiments ($<10^{16}\ \mathrm{cm^{-3}}$), it is assumed that the space charge effects due to the buildup of carriers in the wells is small compared to the applied field. Under these circumstances the electron and hole escape rates

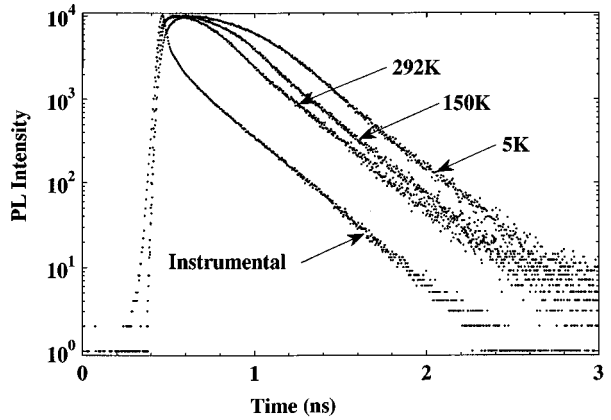

FIG. 2. PL decays spectrally integrated over the peak emission band from a MQW *p-i-n* structure at temperatures of 5, 150, and 292 K, for an internal field of $26\ \mathrm{kV\ cm^{-1}}$. The peak photogenerated carrier density was $<10^{16}\ \mathrm{cm^{-3}}$. The PL decays and the instrumental response shown have been normalized to the same peak count.

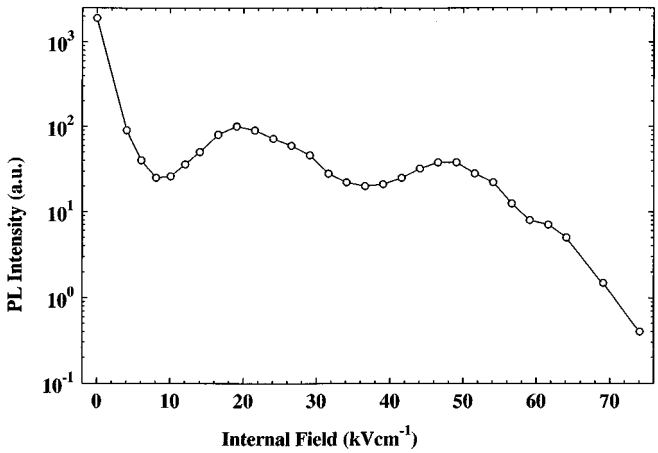

FIG. 4. PL intensity, represented by the PL count rate vs internal field from a GaAs/AlGaAs MQW *p-i-n* structure at a temperature of 5 K. The PL was spectrally integrated over the range 795–805 K which corresponded to the peak of the emission. The lines joining the points are as a guide only.

Downloaded¬04¬Jun¬2002¬to¬137.195.29.233.¬Redistribution¬subject¬to¬AIP¬license¬or¬copyright,¬see¬http://ojps.aip.org/japo/japcr.jsp

from the wells are then linear in carrier density. If it is also assumed that carriers escaping from one well are immediately recaptured by the next well in the direction of carrier motion, then the rate equations for the electron and hole concentrations $n_i(t)$ and $p_i(t)$, respectively, in the ith well are

$$\frac{dn_i(t)}{dt} = \frac{n_{i-1}(t) - n_i(t)}{\tau_n}, \tag{1}$$

$$\frac{dp_i(t)}{dt} = \frac{p_{i+1}(t) - p_i(t)}{\tau_p}, \tag{2}$$

where τ_n and τ_p are the single-well electron and hole emission times. Equations (1) and (2) can be solved analytically for a MQW structure with n_w wells, to give the time dependence of the electron and hole concentrations in each well[25]

$$n_k(t) = \sum_{i=1}^{k} \frac{N_i}{(k-i)!} \left(\frac{t}{\tau_n}\right)^{k-i} \exp\left(-\frac{t}{\tau_n}\right), \tag{3}$$

$$p_k(t) = \sum_{i=k}^{n_w} \frac{P_i}{(i-k)!} \left(\frac{t}{\tau_p}\right)^{i-k} \exp\left(-\frac{t}{\tau_p}\right), \tag{4}$$

where N_i and P_i are the initial excess electron and hole concentrations in the ith well, given simply by Beers law. The time dependence of the PL intensity, $I_{\mathrm{PL}}(t)$, is given by the sum of contributions from each well, thus

$$I_{\mathrm{PL}}(t) = B \sum_{i=1}^{n_w} n_i(t) p_i(t), \tag{5}$$

where B is the radiative recombination coefficient. Equations (3)–(5) can be simplified to give an expression which is dependent only on τ, the reciprocal sum of the electron and hole emission times,

$$I_{\mathrm{PL}}(t) = B \sum_{j=1}^{n_w} \sum_{i=j}^{n_w} \frac{N_j P_i}{(i-j)!} \left(\frac{t}{\tau}\right)^{i-j} \exp\left[-\left(\frac{1}{\tau} + \frac{2}{\tau_{\mathrm{rec}}}\right) t\right], \tag{6}$$

where a linear recombination time τ_{rec} has also been included. Since τ_{rec} can be estimated from measurements of the zero internal field PL decay, the single well escape time τ is the only parameter for variation in the fitting routine.

Figure 5 shows the measured PL decay spectrally integrated over the range 795–805 nm, for the device at a temperature of 50 K with an internal field of 26 kV cm^{-1}. Also shown is the best fit to the model together with the residual distribution, indicating a low scatter of data points around the best fit line, with little systematic deviation. For fields in the range 10–100 kV cm^{-1}, and at all temperatures, the model provides a much closer fit to the experimental data than could be obtained by the common process of fitting the data to an exponential series (as was used for the initial analysis shown in Fig. 3). In Eq. (6), the PL decay is interpreted as the time dependence of the spatial overlap of the electron and hole distributions within the MQW structure. When the carriers are emitted from a quantum well, if they predominantly escaped from the structure without recapture by neighboring wells, then the PL decay would be described by a single exponential function. Since this is clearly not the case for fields <100 kV cm^{-1}, the data provide evidence to support the modeled recapturing process, where carriers emitted by one well have a high probability of recapture by the next well. The model thus provides a convenient means of parametrizing the PL decay in terms of τ, the total escape time from a single well. However, since τ is symmetric in τ_n and τ_p, it does not distinguish between the electron and hole escape times.

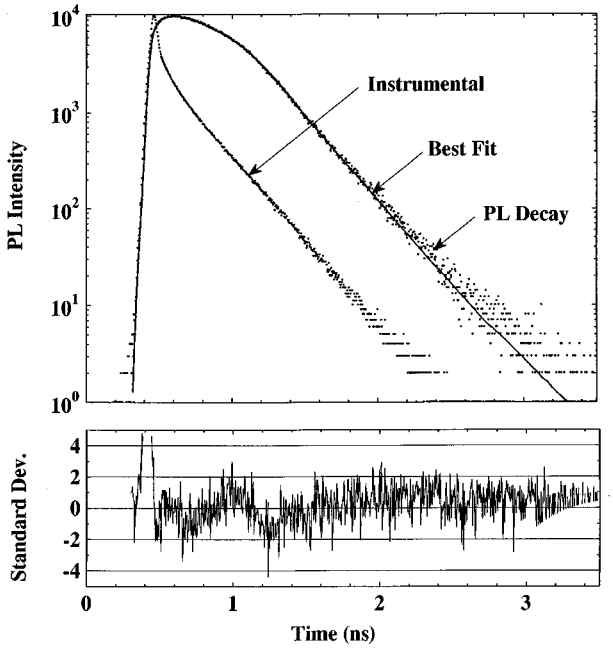

FIG. 5. PL decay from a MQW p-i-n structure spectrally integrated over the range 795–805 nm, for an internal field of 26 kV cm^{-1}, at a temperature of 50 K. The peak photogenerated carrier density was $<10^{16}$ cm^{-3}. The figure also shows the best fit to the decay obtained using the rate equation model, and the corresponding residual distribution. The instrumental response shown has been normalized to the same peak count as the PL decay.

Figure 6 shows a plot of the total escape time τ versus internal field at temperatures of 5, 100, 200, 292, and 350 K. It should be emphasized that τ is the single well escape time and thus it is much shorter than the mean PL decay time. The use of a MQW structure as opposed to a single well increases the complexity of the model, but has the advantage of raising the total PL output from the sample, and also of increasing the overall escape time to within the temporal resolution of the measurement system. As would be expected, Fig. 6 shows similar field and temperature dependences to those observed in Figs. 3 and 4, with the data indicating that the overall PL decay time is a factor of ~ 30 greater than the single well escape time.

IV. DISCUSSION

For deep GaAs/$Al_xGa_{1-x}As$ quantum wells (i.e., $x > 0.2$), there are two mechanisms by which carriers escape in the presence of an electric field: thermionic emission and quantum mechanical tunneling. Schneider and von Klitzing[25] give the thermionic emission time $\tau_{\mathrm{thm}}^{e,h}$ from a quantum well of width L_w at an applied field ϵ as

Downloaded¬04¬Jun¬2002¬to¬137.195.29.233.¬Redistribution¬subject¬to¬AIP¬license¬or¬copyright,¬see¬http://ojps.aip.org/japo/japcr.jsp

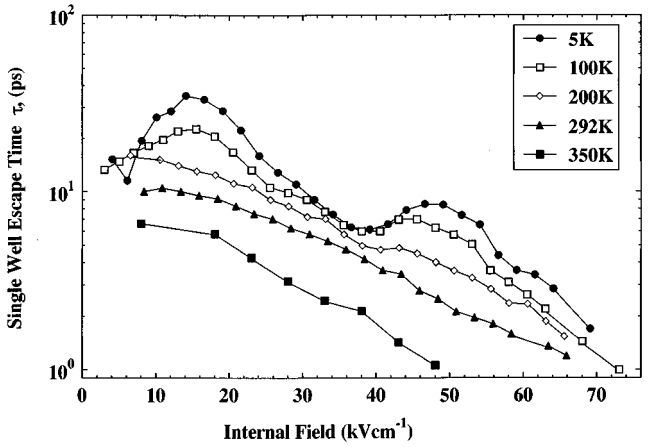

FIG. 6. Single well escape parameter τ versus internal field at temperatures of 5, 100, 200, 292, and 350 K. τ was obtained by fitting each decay to the rate equation model, using reconvolution analysis. The lines joining the points are as a guide only.

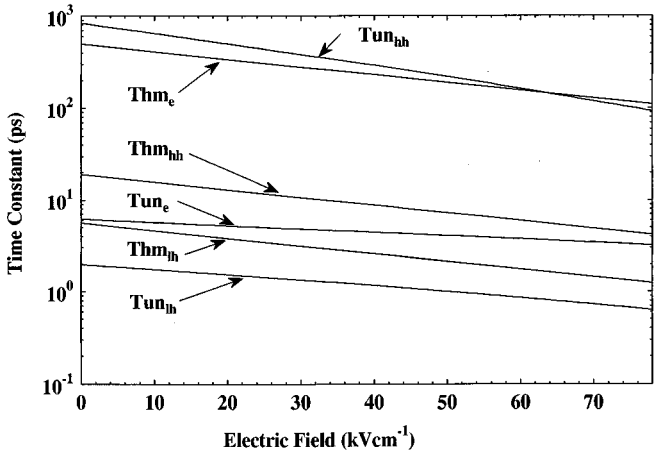

FIG. 7. Calculated single well escape times for electrons, heavy holes and light holes due to thermal emission and nonresonant tunneling. The times were calculated for the structure used in the experiments at room temperature, using Eqs. (7)–(9).

$$\frac{1}{\tau_{\text{thm}}^{e,h}} = \left(\frac{k_B T}{2\pi m_{(e,h)} L_W^2}\right)^{1/2} \exp\left(-\frac{H_{(e,h)}(\epsilon)}{k_B T}\right), \tag{7}$$

where e or h refers to electrons or holes, respectively, m is their effective mass in the well, and T is the absolute temperature. The emission rate is determined by the barrier height, $H(\epsilon)$, over which the particles must be emitted from a bound state in the quantum well, into the continuum of states. $H(\epsilon)$ is given as

$$H_{(e,h)}(\epsilon) = \Delta E_{(c,v)} - E_{(e,h)}^{(n)} - \tfrac{1}{2}|e|\epsilon L_W, \tag{8}$$

where $\Delta E_{c,v}$ is the conduction or valence band offset, depending on whether the particles are electrons or holes, and $E_{(e,h)}^{(n)}$ is the energy of the nth electron (hole) subband, with zero electric field, relative to the bottom of the well.

The quantum mechanical tunneling rate from the nth sublevel has been given by Larsson *et al.*[26] as the product of the barrier collision frequency and the quantum mechanical tunneling probability:

$$\frac{1}{\tau_{\text{tun}}^{e,h}} = \left(\frac{n\hbar\pi}{2L_W^2 m_{e,h}}\right) \exp\left(-\frac{2L_b\sqrt{2m_{b_{e,h}} H'(\epsilon)}}{\hbar}\right), \tag{9}$$

where L_b is the barrier thickness, $m_{b_{e,h}}$ is the particle effective mass in the barrier material, and $H'(\epsilon)$ is the effective barrier height in the presence of an electric field. For the low field case considered in these experiments $H'(\epsilon)$ can be approximated by Eq. (8), with L_W replaced by the MQW period $d(=L_W+L_B)$. Figure 7 shows the electric field dependence of the single well thermionic emission and nonresonant tunneling times for electrons, heavy holes, and light holes calculated using Eqs. (7)–(9) for the structure used in our experiments at room temperature.

For measurements at 5 K, the thermionic emission terms can be neglected when calculating the carrier escape time. In addition, if it is assumed that thermalization of the electrons and holes within the wells is rapid, compared to their escape time from the well, then escape from the $n=1$ light hole and higher electron and hole subbands can also be discounted at this temperature. Thus the dominant transport mechanism may be expected to be the tunneling of $n=1$ electrons and heavy holes. Figures 3, 4, and 6 show pronounced minima at fields of $\sim 6-9$ kV cm^{-1} and $\sim 36-38$ kV cm^{-1}, and a less distinct minimum at a field of ~ 60 kV cm^{-1}. These features are characteristic of resonant tunneling, a process which has been observed in MQW structures by a number of authors.[14–19] The position of the electron and hole energy levels within the wells was estimated for the sample under investigation using the simple square well theory. The estimated energy separation of the $n=1$ heavy hole (hh1) and the $n=1$ light hole (lh1) sub-bands indicates that alignment of these levels in adjacent wells should occur at a field of ~ 10 kV cm^{-1}, while alignment of the $n=1$ and $n=2$ heavy hole (hh2) subbands should occur at a field of ~ 16 kV cm^{-1}. Thus, the feature located at $\sim 6-9$ kV cm^{-1} could be attributed to either process. The energy separation of the $n=1$ and $n=3$ heavy hole sub-bands (hh1–hh3) is estimated to occur at a field of ~ 43 kV cm^{-1}, and corresponds most closely with the second minimum observed in the experimental data at a field of $\sim 36-38$ kV cm^{-1}. Finally, alignment of the $n=1$ and $n=2$ electron sub-bands in adjacent wells should occur at a field of ~ 63 kV cm^{-1} and thus the feature at a field of ~ 60 kV cm^{-1} is most likely associated with this condition.

From the low temperature data in Fig. 6 and the theoretical results in Fig. 7 it is apparent that the calculated electron tunneling times are much shorter, for fields <60 kV cm^{-1}, than the observed values of τ, while the calculated heavy hole tunneling times are much longer. Since τ is mainly determined by the most rapidly escaping carrier species, this implies that Eq. (9) underestimates the electron tunneling time. In addition, the presence of tunneling resonances would be expected to reduce further the observed value of τ below that for the nonresonant case described by Eqs. (7)–(9), consequently providing the structure observed in the field dependence of τ.

The most notable feature in Fig. 6 is the disappearance of the tunneling resonances as the temperature rises above

Downloaded¬04¬Jun¬2002¬to¬137.195.29.233.¬Redistribution¬subject¬to¬AIP¬license¬or¬copyright,¬see¬http://ojps.aip.org/japo/japcr.jsp

~ 150 K. This could be due to frustration of the resonant tunneling process or simply due to the increasing efficiency of thermal processes. Assuming the latter is true, then the magnitude of τ at fields corresponding to the tunneling minima indicates that the resonant and thermal escape processes are comparable at room temperature. As the temperature is increased from 5 K, there is a gradual reduction in the measured τ and the field dependence takes on an approximately exponential form as the tunneling resonances disappear. The room temperature data has a slope of $\sim -40 \times 10^{-3}$ cm kV^{-1} on a semi-logarithmic plot, consistent with the value of $-35 \pm 5 \times 10^{-3}$ cm kV^{-1} obtained by Cavillès *et al.*[13] using a pump-probe technique on asymmetric single quantum well structures. In comparison with the predictions of Eq. (7), the thermal emission times for electrons, heavy holes, and light holes are expected to vary exponentially with field, having a slope at room temperature of $\sim -27 \times 10^{-3}$ cm kV^{-1} on a semi-logarithmic plot. Since the field dependence of τ (Fig. 6) shows a small change in both magnitude and gradient as the temperature is increased from 5 to 292 K then thermal effects must be present at room temperature, however the validity of Eq. (7) for describing this mechanism is not confirmed by the experimental data. Over the range of electric fields used in these experiments, the nonresonant tunneling times calculated using Eq. (9) for electrons, heavy holes, and light holes should also vary approximately exponentially with field. This process, however, would appear to be less likely, since the theoretical field dependence of τ is a poorer fit to the experimental data than the thermionic emission model.

Above room temperature, the carrier escape time and PL intensity decrease considerably suggesting the increasing importance of thermally assisted processes, however a comparison with Eq. (7) indicates an even greater discrepancy with the experimental data. The implication of these results is that the thermionic emission model used to obtain Eq. (7) does not provide an adequate description of the carrier escape from these structures.

The role of thermally assisted processes can be further investigated by observation of the temperature dependence of the PL decay time at each value of electric field, since this should yield information about the activation energy of the process via the Boltzmann equation. Figure 8 shows the activation energies obtained from least squares fits to the data for temperatures $\geqslant 125$ K. The field dependence of the activation energy appears to follow that of the low temperature PL decay time, with minima observed near the resonant tunneling fields, even though the least squares fitting was only performed for higher temperatures. The gradient of Fig. 8 in the region of negative slope is ~ 11 meV cm kV^{-1} and is comparable to the expected energy change per unit field of ~ 13.5 meV cm kV^{-1} over one period of this MQW structure. Extrapolation of this linear region to zero internal field gives an energy of ~ 36 meV, significantly lower than the conduction and valence band offsets of ~ 251 and ~ 124 meV, respectively, and would seem to indicate a much lower barrier for this structure.

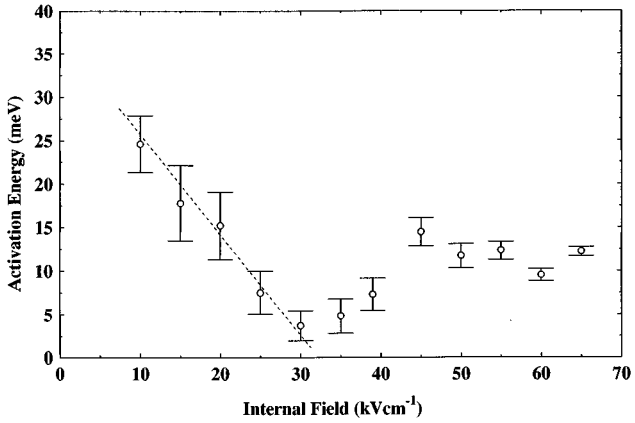

FIG. 8. Activation energy for the thermally assisted escape of carriers from a GaAs/AlGaAs MQW structure, as a function of electric field. The dotted line indicates a straight line fit to the data, having a slope of ~ 13.5 meV cm kV^{-1} and an intercept of ~ 36 meV.

V. CONCLUSIONS

To conclude, TRPL has been used so study the cross-well carrier dynamics in biased MQW *p-i-n* structures at temperatures in the range 5–350 K. The PL decay data have been parametrized by fitting to a linear coupled rate equation model using reconvolution analysis and they provide evidence for a process of successive recapturing of carriers by adjacent wells during the sweepout process. At temperatures <100 K and fields <60 kV cm^{-1} carrier escape appears to be strongly influenced by resonant tunneling between hole subbands in adjacent wells. At higher temperatures, thermally assisted carrier escape becomes more important but does not agree well with conventional thermionic emission models.

ACKNOWLEDGMENTS

The authors acknowledge the support of the Royal Society Paul Instrument Fund and the UK Engineering and Physical Sciences Research Council (EPSRC). The Q-switched laser diodes were supplied by E. L. Portnoi and co-workers, A. F. Ioffe Institute, St. Petersburg. The actively quenched SPADs are used by agreement of S. Cova and co-workers, Polytechnico di Milano, Italy.

[1] T. H. Wood, C. A. Burrus, D. A. B. Miller, D. S. Chemla, T. C. Damen, A. C. Gossard, and W. Wiegmann, Appl. Phys. Lett. **44**, 16 (1984).
[2] D. A. B. Miller, D. S. Chemla, T. C. Damen, A. C. Gossard, W. Wiegmann, T. H. Wood, and C. A. Burrus, Appl. Phys. Lett. **45**, 13 (1984).
[3] A. L. Lentine, H. S. Hinton, D. A. B. Miller, J. E. Henry, J. E. Cunningham, and L. M. F. Chirovsky, Appl. Phys. Lett. **52**, 1419 (1988).
[4] L. L. Chang, L. Esaki, and R. Tsu, Appl. Phys. Lett. **24**, 593 (1974).
[5] E. E. Mendez, W. I. Wang, B. Ricco, and L. Esaki, Appl. Phys. Lett. **47**, 415 (1985).
[6] M. K. Jackson, M. B. Johnson, D. H. Chow, T. C. McGill, and C. W. Nieh, Appl. Phys. Lett. **54**, 552 (1989).
[7] S. Charbonneau, J. F. Young, and A. J. SpringThorpe, Appl. Phys. Lett. **57**, 264 (1990).
[8] D. Y. Oberli, J. Shah, T. C. Damen, C. W. Tu, T. Y. Chang, D. A. B. Miller, J. E. Henry, R. F. Kopf, N. Sauer, and A. E. DiGiovanni, Phys. Rev. B **40**, 3028 (1989).
[9] H. Sakaki, T. Matsusue, and M. Tsuchiya, IEEE J. Quantum Electron. **25**, 2498 (1989).

Downloaded¬04¬Jun¬2002¬to¬137.195.29.233.¬Redistribution¬subject¬to¬AIP¬license¬or¬copyright,¬see¬http://ojps.aip.org/japo/japcr.jsp

[10] M. Nido, M. G. W. Alexander, W. W. Rühle, T. Schweizer, and K. Köhler, Appl. Phys. Lett. **56**, 355 (1990).
[11] K. Leo, J. Shah, E. O. Göbel, T. C. Damen, K. Köhler, and P. Ganser, Appl. Phys. Lett. **56**, 2031 (1990).
[12] K. Leo, J. Shah, J. P. Gordon, T. C. Damen, D. A. B. Miller, C. W. Tu, and J. E. Cunningham, Phys. Rev. B **42**, 7065 (1990).
[13] J. A. Cavaillès, D. A. B. Miller, J. E. Cunningham, P Li Kam Wa, and A. Miller, IEEE J. Quantum Electron. **28**, 3486 (1992).
[14] S. Tarucha, K. Ploog, and K. von Klitzing, Phys. Rev. B **36**, 4558 (1987).
[15] H. Schneider, H. T. Grahn, K. von Klitzing, and K. Ploog, Phys. Rev. B **40**, 10 040 (1989).
[16] G. Livescu, A. M. Fox, D. A. B. Miller, T. Sizer, W. H. Knox, J. E. Cunningham, A. C. Gossard, and J. H. English, Semicond. Sci. Technol. **5**, 549 (1990).
[17] A. M. Fox, D. A. B. Miller, G. Livescu, J. E. Cunningham, and W. Y. Jan, IEEE J. Quantum Electron. **27**, 2281 (1991).
[18] D. C. Hutchings, C. B. Park, and A. Miller, Appl. Phys. Lett. **59**, 3009 (1991).
[19] A. Miller, C. B. Park, and P. LiKam Wa, Appl. Phys. Lett. **60**, 97 (1992).
[20] G. S. Buller, J. S. Massa, and A. C. Walker, Rev. Sci. Instrum. **63**, 2994 (1992).
[21] Z. I. Alferov, A. B. Zuravlev, E. L. Portnoi, and N. M. Stel'makh, Sov. Tech. Phys. Lett. **12**, 452 (1986).
[22] A. Lacaita, M. Ghioni, and S. Cova, Electron. Lett. **25**, 841 (1989).
[23] J. S. Massa, G. S. Buller, A. C. Walker, J. L. Oudar, E. V. K. Rao, B. G. Sfez, and R. Kuselewicz, Appl. Phys. Lett. **61**, 2205 (1992).
[24] D. V. O'Connor and D. Phillips, *Time-Correlated Single Photon Counting* (Academic, New York, 1983).
[25] H. Schneider and K. von Klitzing, Phys. Rev. B **38**, 6160 (1988).
[26] A. Larsson, P. A. Andrekson, S. T. Eng, and A. Yariv, IEEE J. Quantum Electron. **24**, 787 (1988).

Downloaded¬04¬Jun¬2002¬to¬137.195.29.233.¬Redistribution¬subject¬to¬AIP¬license¬or¬copyright,¬see¬http://ojps.aip.org/japo/japcr.jsp